

Preparation of Ti6Al4V Powder with High Yield of Fine Particle by Crucible-less Gas Atomization Technology

Zai Xiongfei, Chen Shiqi, Liu Yong, Li Ruidi, Wu Hong

State Key Laboratory of Powder Metallurgy, Central South University, Changsha 410083, China

Abstract: This study aims at producing sphere Ti6Al4V powders with tailed physical characteristics for additive manufacturing application. Ti6Al4V powders were prepared by a novel electrode induction guiding gas atomization (EIGA) equipment designed independently. The yielding rate of fine powders could be improved by reasonably increasing feed rate and atomization gas pressure. Interestingly, the yield (35%) of powder particles below 45 μm by EIGA is significantly higher than the yield (~10%) by conventional plasma rotating electrode technology. The powder properties and microstructure were characterized by scanning electron microscope (SEM), X ray diffraction (XRD) and optical microscope (OM). The powders exhibited satisfactory flowability and high apparent density for good sphericity and smooth surface. The powders with tailed size ranges could be used for various additive manufacturing methods and injection moulding etc. The β phase of Ti6Al4V translates to needle-like α' phase during atomization process because of the fast cooling rate calculated to be $10^4\sim 10^8$ K/s.

Key words: Ti6Al4V powders; gas atomization; microstructure; additive manufacturing; cooling rate

Recently, metal additive manufacturing has been widely investigated all around the world, which has been widely used in aerospace, chemical industry and medical device etc. This emerging manufacturing technology not only enables products with complex geometry shape, but also can prepare products without mould, and thus the development cycle is shortened and utilization ratio of raw materials improved^[1-4]. Up to now, metal materials such as 316L^[5], AlSi12^[6], Inconel 718^[7,8], Co-Cr^[9], and Ti6Al4V^[10-12] have been widely used for powder bed or powder deposition additive manufacturing technologies. Above two methods have different demands for metal powder particle size. For powder bed additive manufacturing, the metal powder particle size should be usually below 45 μm ^[13-15]. While for deposition additive manufacturing, the powder size should be 45~150 μm ^[16,17]. A few researches about the preparation of metal powder and relevant physical properties for additive manufacturing were reported^[18].

Titanium and its alloy have many particular characteristics, such as low density, high strength weight ratio, fasci-

nating corrosion resistance and lower Young's modulus. Thus, titanium and its alloy are widely used in many fields, especially the additive manufacturing, which possesses considerable market demand for suitable powder^[19-21]. However, a challenge of additive manufacturing titanium and its alloy is the production of high purity spherical powders, owing to the high reactivity between titanium and crucible (Al_2O_3)^[22]. Up to now, titanium and its alloy powders are usually prepared by the following methods without crucible: plasma rotating electrode process (PREP)^[23], multi-torch plasma wire atomization (PWA)^[22], plasma melting inducting gas atomization (PIGA), electrode induction guiding gas atomization (EIGA)^[24] and combustion reaction^[25]. However, PREP produces very low yields (~10%) of ~45 μm powders, which is not suitable for powder bed additive manufacturing. PWA and PIGA produce powders with high costs of production rate, equipment costs and energy efficiency. The powders produced by combustion reaction have high oxygen content (0.5wt%~1.5wt%). The EIGA method has satisfactory yields (~35%) of ~45 μm pow-

Received date: June 25, 2018

Corresponding author: Chen Shiqi, Professor, Central South University, Changsha 410083, P. R. China, Tel: 0086-731-88830464, E-mail: chenpm450@163.com

Copyright © 2019, Northwest Institute for Nonferrous Metal Research. Published by Science Press. All rights reserved.

ders and relatively acceptable costs. This method holds great potential in titanium and its alloy powder production.

EIGA process is certainly different from conventional gas atomization methods for the discontinuous metal liquid flow and extremely low superheat (about 10 °C). To the best knowledge of the authors, the reports on EIGA process and relevant powder properties, especially the preparation of Ti6Al4V powder, are few. In this research, we reported the preparation of Ti6Al4V powder by EIGA method. The effects of the atomization parameters on the powders size distribution were discussed. The properties and microstructural evolution of Ti6Al4V powders were characterized. The cooling rate was also calculated to explain the phase composition.

1 Experiment

The schematic diagram of the EIGA equipment designed independently is shown in Fig.1. The titanium alloy bar is rotated into the induction coil and melted to metal droplets. Under the mutual effects of gravity and gas field, the droplets fall into the atomization tower through guiding nozzle and then are atomized by the high pressure argon gas. At last, the powders are collected by powder collection chamber.

The Ti6Al4V powders were prepared with different atomization parameters, as shown in Table 1. The powders size distribution was obtained by the particle size analysis with screens. Then the powders were sieved into two different fractions. One fraction with a particle size ranging from 10 to 45 μm can be used for selective laser melting (SLM). The other fraction with a particle size ranging from 45 to 150 μm can be used for laser engineered net shaping (LENS) and electron beam selective melting (EBSM). The flowability and apparent density of the powders ranging from 45 to 150 μm were measured by Hall-flowmeter equipped with a 25 mL container^[26]. The powder chemical component was analyzed by inductively coupled plasma atomic emission spectrometry (ICP-AES) and oxygen nitrogen hydrogen analyzer. The surface morphology and sphericity were observed by SEM. The microstructure of the powders was characterized with OM and XRD.

2 Results and discussion

2.1 Effects of atomization parameters on powder size distribution

2.1.1 Effect of feed rate on powder size distribution

The Ti6Al4V powders were prepared by different alloy bar feed rates with constant atomization gas pressure of 4 MPa. The powder size distributions under different feed rates were shown in Fig.2. It can be seen that the yielding rate of fine powders increases with the increase of feed rate in the EIGA process. The yielding rate of powders size below 45 μm was about 35% and power supply reached to

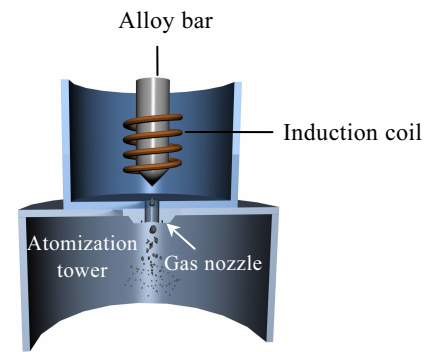


Fig.1 Schematic sketch of an EIGA process

Table 1 Atomization processing parameters

Powder	Feed rate/mm·min ⁻¹	Atomization pressure/MPa
a	25	4.0
b	30	4.0
c	35	4.0
d	40	4.0
e	40	3.5

maximum power when the feed rate was 40 mm/min. The raw materials can not be completely melted and the process would be unstable when the feed rate is beyond 40 mm/min for the limit of heating power. However, for the traditional gas atomization, it is well known that the powder size increases with the increase of feed rate. The reason can be explained by the following mechanism.

Time (t) of droplet from bar to atomization section could be calculated by the formula (Newton second law of motion):

$$t = \frac{\sqrt{v^2 + 2aH} - v}{a} \quad (1)$$

Where v is the feed rate, a is the acceleration of droplet, H is the distance from the bar melting head to atomization section.

As the feed rate v increases, the t decreases, which ultimately leads to the less heat loss. As a result, under a rapid feed rate, the droplet possesses high atomization temperature and low viscosity, which is helpful for the melt droplets being fully broken into fine particles.

2.1.2 Effect of atomization gas pressure on powder size distribution

The size distribution of powders prepared with different atomization pressures is shown in Fig.3, under the feed rate fixed at 40 mm/min. The yield of fine powders increases with the increase of atomization pressure, due to the transformation of motion energy of argon gas into the surface

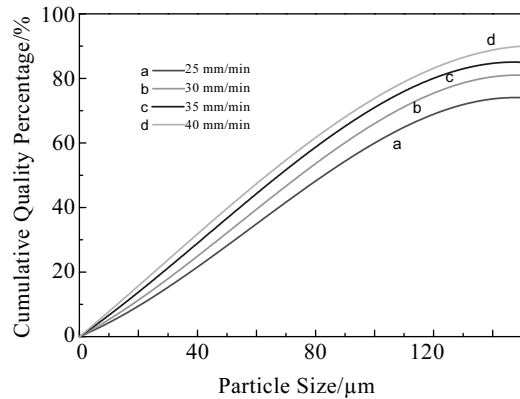


Fig.2 Powder particle size distribution with different feed rate, $P = 4$ MPa

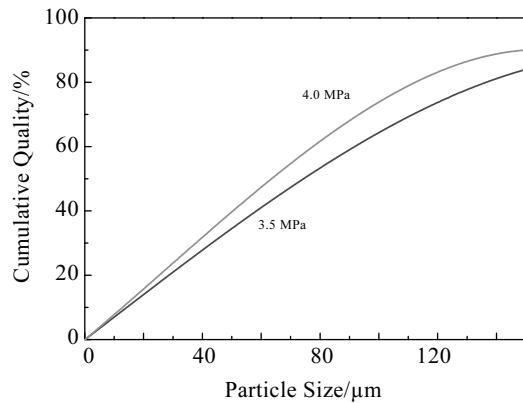


Fig.3 Powder particle size distribution with different atomization pressures when the feed rate is 40 mm/min

energy of powders. The median particle size d_m decreased from 73 μm to 62 μm when atomization gas pressure increased from 3.5 MPa to 4.0 MPa. Median particle size d_m can be calculated by the following equation^[27]:

$$d_m = KF^{-1/2} \quad (2)$$

where K is a constant and F is the specific gas consumption in m^3/kg . The value of K is a function of nozzle design and alloy properties.

For a certain atomization nozzle, enhancing the atomization gas supply pressure favors gas mass flow and gas consumption. Consequently, d_m decreases with increase of the atomization gas supply pressure.

2.2 Powder characterization

The chemical composition of powders and raw material indicates that various element contents all meet the standard demand, as shown in Table 2. The atomization temperature is higher than Ti6Al4V melting point (1670 $^{\circ}\text{C}$) and the melting time is relatively short, so that the elements burning

Table 2 Chemical composition of raw material and as-prepared powder (mass fraction)

Element	Nominal composition	Raw material	Powders
Ti	Balance	Balance	Balance
Al	5.5%~6.75%	6.25%	6.22%
V	3.5%~4.5%	4.38%	4.38%
Fe	$\leq 0.3\%$	0.15%	0.14%
C	$\leq 0.1\%$	0.019%	0.019%
O	$\leq 1600 \mu\text{g}\cdot\text{g}^{-1}$	$600 \mu\text{g}\cdot\text{g}^{-1}$	$\leq 1500 \mu\text{g}\cdot\text{g}^{-1}$
N	$\leq 300 \mu\text{g}\cdot\text{g}^{-1}$	$16 \mu\text{g}\cdot\text{g}^{-1}$	$16 \mu\text{g}\cdot\text{g}^{-1}$
H	$\leq 125 \mu\text{g}\cdot\text{g}^{-1}$	$74 \mu\text{g}\cdot\text{g}^{-1}$	$74 \mu\text{g}\cdot\text{g}^{-1}$

loss is very few during the process. The oxygen content can be controlled under a satisfied standard for the argon protective atmosphere. The oxygen content of powders ranging from 45 to 150 μm could be controlled below $1000 \mu\text{g}\cdot\text{g}^{-1}$. The oxygen content of powders size below 45 μm was about $1500 \mu\text{g}\cdot\text{g}^{-1}$ because of the more specific surface area.

Powder particles have good sphericity and smooth surface observed from SEM images (Fig.4), although little imperfect sphericity and satellite powders are present. The satellite powders are due to collision between particles in flight during atomization process. Generally, the satellite powders by EIGA atomization process are smaller than by traditional gas atomization, because the metal droplets are not continuous during EIGA process, leading to the relatively lower concentration of powders in the atomization tower compared with traditional gas atomization.

Powders ranging from 45 to 150 μm have excellent flowability (24.3 s/50 g) and high apparent density ($2.579 \text{ g}/\text{cm}^3$), which can guarantee the laser deposition additive manufacturing. Powders ranging from 10 to 45 μm have satisfactory flowability which ensures the powder layer uniformity of powder bed additive manufacturing.

Internal pores are presented in Fig.5. This phenomenon is common in gas atomization for gas entrapment. The internal pores reduce the tap density. Moreover, the internal pores usually decrease the density and mechanical property in thermal spray deposition, additive manufacturing productions etc. By region counting, powders with internal pores account for only about 2% in powders ranging from 45 to 150 μm . The percent (about 3%) of powders with internal pores in powders below 45 μm is higher owing to the faster cooling rate.

Ti6Al4V is a typical dual phase titanium alloy. However, the XRD peaks observed in Fig.6 are typical hexagonal close-packed structure of Ti without peaks of β phase. It is because the rapid cooling process begins above martensite phase transformation temperature, and thus β phase transforms into needle-like α' phase, as shown in Fig.7. The following section will calculate the cooling rate to elucidate the microstructural formation.

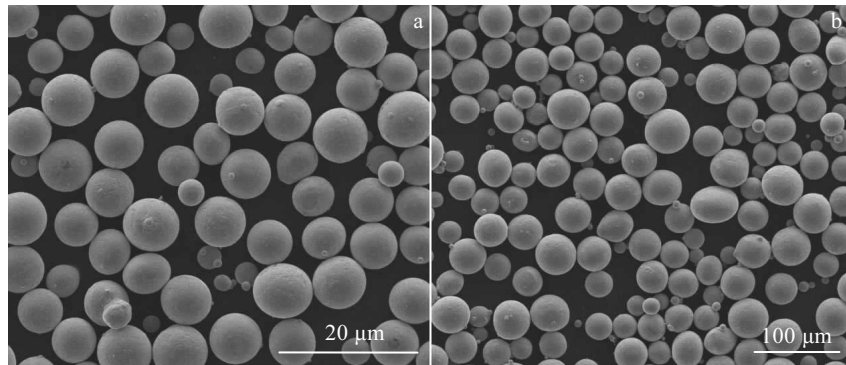


Fig.4 SEM images showing the surface morphologies of EIGA powder: (a) 45~150 μm and (b) <45 μm

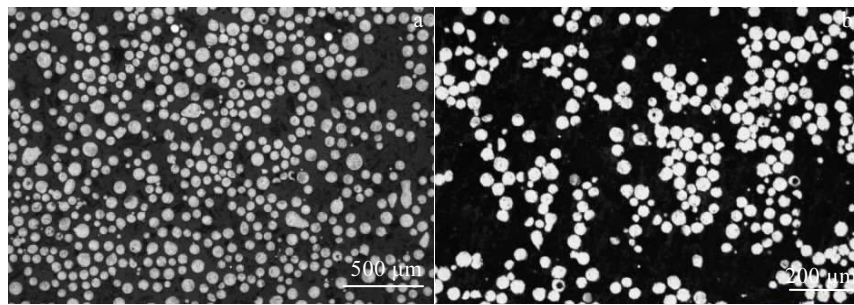


Fig.5 OM images showing the powder cross section: (a) 45~150 μm and (b) <45 μm

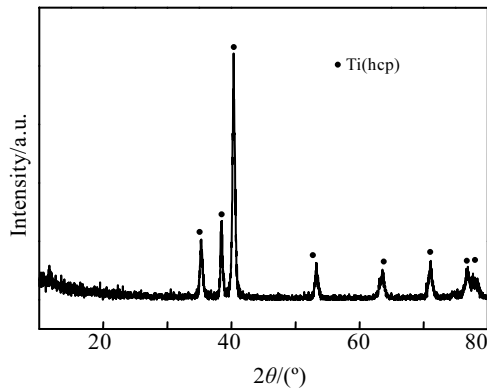


Fig.6 X-ray diffraction pattern of the powders

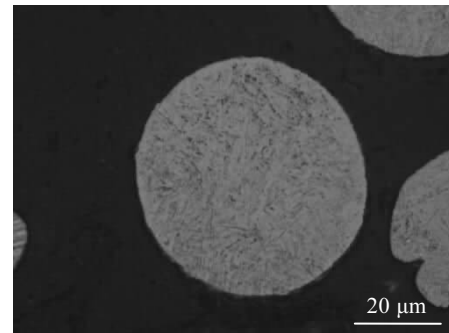


Fig.7 OM image of powder showing the needle-like α' phase

2.3 Calculation of cooling and solidification rates

According to Ref.[28, 29], the heat transfer coefficient (h) between the argon and droplet during process can be calculated as follows:

$$h = 2 \frac{K_w}{D} + 0.6K_w \left(\frac{\rho_w |v_d - v_w|}{\mu_w D} \right)^{1/2} P_r^{1/3} \quad (3)$$

where K_w is thermal conductivity of the gas ($W \cdot m^{-1} \cdot K^{-1}$), D the diameter of a droplet, P_r is the Prandtl number, v_d and v_w are the velocities for the melt drop and the gas ($m \cdot s^{-1}$), respectively, ρ_w is density of the gas ($kg \cdot m^{-3}$), μ_w is kinetic

viscosity of the gas ($kg \cdot m^{-1} \cdot s^{-1}$).

During the atomization, v_d is roughly equal to v_w , so that

$$h = 2 \frac{K_w}{D} \quad (4)$$

According to Ref.[30], the cooling rate v_c can be calculated by the formula

$$\frac{dT_d}{dt} = \frac{hA(T_d - T_e)}{\rho V C_p} \quad (5)$$

Where V is volume (m^3), ρ is density ($kg \cdot m^{-3}$), C_p is specific heat capacity ($J \cdot kg^{-1} \cdot K^{-1}$), A is surface area of the melt drop

(m^2), T_d and T_e are melt drop temperature (K) and environment temperature (K), t is time (s).

Applying Eq. (4) and parameters to Eq. (5), the cooling rate can be calculated as follows:

$$\frac{dT_d}{dt} = \frac{12K_w(T_d - T_e)}{\rho C_p D^2} \approx 19.2 \times \frac{1}{D^2} \quad (6)$$

Where $K_w=3.55 \times 10^{-4} \text{ J} \cdot \text{cm}^{-1} \cdot \text{K}^{-1} \cdot \text{s}^{-1}$, $T_d=1913.15 \text{ K}$, $T_e=300 \text{ K}$, $\rho=4.5 \text{ g} \cdot \text{cm}^{-3}$, $C_p=7.955 \text{ W} \cdot \text{K} \cdot \text{m}^{-1}$

The cooling rate is estimated to be about $10^4 \sim 10^8 \text{ K/s}$ during the atomization. Consequently, the fast cooling rate contributes to the needle-like α' phase formation.

3 Conclusions

1) The yield of fine powders could be increased by using a higher feed rate and gas pressure. The yield of $\sim 45 \mu\text{m}$ powders could reach to 35% under the optimal technological condition of feed rate 40 mm/min and gas pressure 4.0 MPa.

2) The Ti6Al4V powders prepared by EIGA equipment meet the standard demands for additive manufacturing in aspects of chemical component, size distribution, flowability and apparent density. The powders ranging from 45 to 150 μm have satisfactory flowability (24.3 s/50 g) and high apparent density (2.579 g/cm^3) which can be used for deposition additive manufacturing. Powders ranging from 10 to 45 μm have satisfactory flowability which ensures the powder layer uniformity of powder bed additive manufacturing.

3) During gas atomization process, the β phase in droplets translates to needle-like α' phase in powder particle owing to the fast cooling rate ($10^4 \sim 10^8 \text{ K/s}$) during the gas atomization.

References

- Wohlers. *Wohlers Report 2013*[R]. Fort Collins, Colorado, USA: Wohlers Associates Inc, 2013
- Zhai Y, Lados D A, LaGoy J L. *JOM*[J], 2014, 66: 808
- Frazier W. *Mater Eng Perform*[J], 2014, 23: 1917
- Wauthle R, Vander Stok J, Yavari S A et al. *Acta Biomater*[J], 2015, 14: 217
- Yan C, Hao L, Hussein A et al. *Mater Des*[J], 2014, 55: 533
- Li X P, Wang X J, Saunders M et al. *Acta Mater*[J], 2015, 95: 74
- Amato K N, Gaytan S M, Murr L E et al. *Acta Materialia*[J], 2012, 60: 2229
- Zhao X, Chen J, Lin X et al. *Materials Science and Engineering A*[J], 2008, 478: 119
- Koutsoukis T, Zinelis S, Eliades G et al. *J Prosthodont*[J], 2015, 24: 303
- Thijs L, Verhaeghe F, Craeghs T et al. *Acta Materialia*[J], 2010, 58: 3303
- Vrancken B, Thijs L, Kruth J P et al. *Journal of Alloys and Compounds*[J], 2012, 541: 177
- Hollander D A, Von Walter M, Wirtz T et al. *Biomaterials*[J], 2006, 27: 955
- Xu W, Brandt M, Sun S et al. *Acta Materialia*[J], 2015, 85: 74
- Li R, Shi Y, Wang Z et al. *Applied Surface Science*[J], 2010, 256: 4350
- Dadbakhsh S, Hao L, Jerrard P G E et al. *Powder Technology*[J], 2012, 231: 112
- Raju R, Duraiselvam M, Petley V et al. *Materials Science and Engineering: A*[J], 2015, 643: 64
- Hua T, Jing C, Xin L et al. *Journal of Materials Processing Technology*[J], 2008, 198: 454
- Yablokova G, Speirs M, Van Humbeeck J et al. *Powder Technology*[J], 2015, 283: 199
- Yadroitsev I, Krakhmalev P, Yadroitsava I. *Journal of Alloys and Compounds*[J], 2014, 583: 404
- Murr L E, Quinones S A, Gaytan S M et al. *J Mech Behav Biomed Mater*[J], 2009(2): 20
- Welsch B R ed. *Materials Properties Handbook: Titanium Alloys*[M]. Ohio: ASM international, 1993
- Antony L V M, Reddy R G. *Jom-J Min Met Mat S*[J], 2003, 55: 14
- Tokizane M, Isonishi K. *J Jpn Soc Powder Powder Metallurgy*[J], 1992, 39: 1137
- Hohmann M. *Advances in Powder Metallurgy*[J], 1992(1): 27
- Nersisyan H H, Yoo B U, Kim Y M et al. *Chemical Engineering Journal*[J], 2016, 304: 232
- Vlachos N, Chang I T H. *Powder Technology*[J], 2011, 205: 71
- Alan Lawley. *Atomization*[M]. New Jersey: Metal Powder Industries Federation, 1992: 74
- Szekely J, Themelis N J. *Rate Phenomena in Process Metallurgy*[M]. New York: Wiley-Interscience, 1971
- Estrada J L, Duszczczyk J. *Journal of Materials Science*[J], 1990, 25: 1381
- Holman J P. *Heat Transfer, 8th Edition*[M]. New York: McGraw-Hill, 1997

无坩埚熔炼气雾化技术制备 Ti6Al4V 粉末

宰雄飞, 陈仕奇, 刘咏, 李瑞迪, 吴宏

(中南大学 粉末冶金国家重点实验室, 湖南 长沙 410083)

摘要: 采用自主研发设计的无坩埚熔炼气雾化设备制备适用于金属增材制造的球形Ti6Al4V粉末。通过调节进料速度与雾化压力, 45 μm 以下的粉末收得率可达35%(质量分数), 高于旋转电极制粉的收得率(~10%)通过扫描电子显微镜(SEM)、X射线衍射(XRD)和金相显微镜(OM)表征粉末显微结构与组织。结果表明制备的Ti6Al4V粉末具有良好的球形度和表面光滑, 良好的流动性和较高的松装密度使其可用于金属增材制造与注射成型等。由于雾化过程中粉末的冷却速度为 $10^4\sim 10^8$ K/s, 粉末中的 β 相在冷却过程中转变为针状 α' 相。

关键词: Ti6Al4V粉末; 气雾化; 显微结构; 增材制造; 冷却速度

作者简介: 宰雄飞, 男, 1992年生, 硕士生, 中南大学粉末冶金研究院, 湖南长沙 410083, 电话: 0731-88830464, E-mail: zxf735@163.com